

T.2: Electron beam orbit control systems for Synchrotron Radiation Sources and Indus-2: A perspective

R.P. Yadav and P. Fatnani

(*rpyadav@rrcat.gov.in*)

Accelerator Controls Section

Accelerator Controls & Beam Diagnostics Division

(On behalf of the working group on fast orbit feedback system for Indus-2)

Introduction

Indus-2 is a 2.5 GeV Synchrotron Radiation Source (SRS) with 12 beamlines under various stages of operation. The electron beam orbit in such an SRS gets affected due to factors like dipole field errors, magnet alignment errors, slow power supply drifts, ground settlements, ground vibrations, thermal expansion of components, insertion devices open/close operation, etc. The perturbed orbit may result in the changes in the position of the SR light spot at the front-end of beam lines, which reduces the effective flux and brightness of the light going into the beam line and affects the experiment at the corresponding experimental station. So this needs to be corrected. Depending upon the orbit distortion types, their sources and nature, different orbit correction schemes are used at different SRS facilities all around the world. Depending upon the localization or spread of the electron beam position error sensing and correction effort applied, the orbit correction methods are categorized into local and global orbit correction schemes. Local orbit correction schemes utilize the beam position error data collected from the nearby Beam Position Indicators (BPIs) for calculating the corrector strength values to be applied to the corrector in closed loop feedback scheme. This results in a very fast corrective action as both the position error measurement devices (BPI) as well as the correcting actuators are in near vicinity to each other. Also the relatively less number of inputs and outputs (typically 2-4 BPIs and 3-4 correctors) result in reduced complexity of controller which is favorable from implementation and tuning point of view. Typically, several beam lines will have such local orbit correction loops implemented. However, mutual coupling among the loops is a big issue. With degradation in the effectiveness of orbit bump closure condition due to the BPI errors, modeling errors / system model variations arising due to different reasons, mutual coupling of different local loops may occur that reduces its effectiveness. The global correction schemes are good at addressing the modeling errors and model

mismatches as these are based on the algorithms that try to correct the beam position errors spread all over the orbit at an instant of time. As a result these schemes require the beam position data from all the BPIs to be made available to the controller for calculating the corrector values in feedback form. With the larger number of inputs and outputs to be handled by the controller, these schemes incorporate complex controllers with distributed calculation features (mostly for FOFB schemes). From the point of view of loop correction timing, the electron orbit correction systems are categorized into 'slow orbit feedback' correction systems with typical correction rates employed of the order of few Hz (< 5 Hz, $\sim .05$ to 1 Hz) and 'fast orbit feedback' correction systems with correction rates up to few kHz. Global slow orbit correction schemes are employed for correcting the orbit distortion occurring at slower intervals, like the electron orbit variations arising out of thermal drifts, ground settlements and power supply drifts. Fast orbit correction aims at correcting much faster orbit oscillations (5Hz to 200 Hz), essentially due to noise coupled from ground vibrations into the system through mechanical vibrations of lattice magnets, power supply ripple, booster cycles during top-up injection and insertion device gap-phase reconfiguration. Mostly all of these schemes work on the error feedback based correction mechanism, by taking feedback from beam position indicators, calculating required correction strengths and applying them on corrector magnets. The choice of FOFB parameters are primarily governed by type of noise present at the site location and the machine design. Table T.2.1 lists the typical electron beam movement sources found in SRS machines [1, 2] and table 2 lists typical FOFB system design parameters of some of the SRS machines.

Table T.2.1: Typical electron beam movement sources in SRS

Sr. No.	Source	Approximate amplitude order	Time scale
1	Ground settlement	~ mm	weeks-years
2	Seasonal ground motion	< mm	weeks-years
3	Diurnal temperature	1-100 μ m	minutes-days
4	River, dam activity	1-100 μ m	minutes-days
5	Crane motion	1-100 μ m	minutes-days
6	Machine related Component heating BPM intensity dependence Filling patterns	1-100 μ m	minutes-days

7	Ground Vibrations, traffic movement, train movement etc	< μm	milliseconds-seconds
8	Cooling water vibrations	$\sim\mu\text{m}$	
9	Booster operation	$\sim\mu\text{m}$	
10	Air conditioners , pumps	$\sim\mu\text{m}$	
11	Power supplies	$\sim\mu\text{m}$	
12	Insertion device jaw movement	1-100 μm	
13	Vacuum chamber vibration from BL shutters and valve operations.	$\sim\mu\text{m}$	
14	Pulsed power sources	$\sim\mu\text{m}$	sub-milliseconds
15	Synchrotron oscillations	1-100 μm	
16	Single and multi-bunch instabilities	1-100 μm	

- Targeted by SOFB systems
- Targeted by FOFB systems
- Correction of these requires special feedback control systems

Typical electron beam movements observed in SRS

Some of the most commonly occurring sources of electron beam instability in synchrotron radiation sources are listed in the Table T.2.1. These noise sources cause beam motion over a broad range of time scale ranging from years to sub-milliseconds, with different orders of disturbance amplitudes. Also, mostly this amplitude is of decreasing nature with increasing frequency (Fig. T.2.1). Long-term motion generally caused by ground settlements and seasonal temperature changes does not pose problem to users since experiments are regularly re-aligned. But these changes can alter the circumference of large rings by few tens of microns which is not desirable from machine side as this enforces the machine realignment requirements. For correcting the ill effect from these types of motions, the method of stabilizing the tunnel ring temperature and cooling water temperature up to 0.1- 0.3 °C is utilized. Along with this the technique of average orbit correction in horizontal plane with RF frequency compensation is also used in many machines. Practice of utilizing the temperature stable materials such as Invar or carbon fiber to support critical components (beam position monitors) is another common method employed towards this. Policy of machine design considering injection at full energy to avoid magnet ramping is also supported in favor of this.

Table T.2.2: FOFB design parameters of different SRS facilities

SR facility	Max BW	Stability (rms)	Loop rate (KHz)	BPI electronics Type & BW	DAC
ALS	<50 Hz	<1 μm	1.1	Bergoz type, multiplexed	effective 20Bits
APS	50 Hz	<1 μm	1.5	Custom, 5 KHz	16Bit
BESSY	<100Hz	<1 μm	2.4	Analog, 2.5 KHz	19 Bits, ADC 16 bits
ESRF	150 Hz	<0.6 μm	10	Libera, 10KHz
Indus-2	100 Hz	<2 μm	5	Libera, 10KHz	16bits
DIAMOND	150Hz	0.2 μm	\sim 10	Libera, 10KHz	24bit
SOLEIL	150Hz	0.2 μm	<3.5	Libera, 10KHz	16bits
NSLS	< 200Hz	1.5 μm	<5	Custom HW	18Bits

Medium-term motion primarily in the range of minutes to seconds is the one targeted by slow orbit feedback systems for corrections. For mitigating these passive effects and their correction, methods like selecting the design that avoids the natural frequencies of girders near to ground vibration frequencies, physical isolation of vibration sources from ground or accelerator structure using damping support materials, selecting lattice design that supports grouping of focusing and defocusing quadrupoles together as a rigid body to girders that are mounted and aligned as a single unit so that whenever there is a movement they move together are employed.

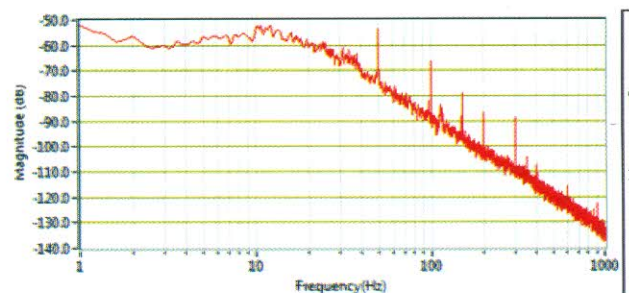


Fig. T.2.1 : FFT of beam noise measured at Indus-2 BPI (RMS average of 10 datasets with Hanning window applied)

Residual beam orbit vibrations that cannot be corrected by the above passive methods to the desired levels in this frequency range are then aimed by the fast orbit feedback systems for correction to the desired limits. The beam orbit movements of the order of sub-millisecond level do not come under the scope of orbit feedback control systems and are corrected using the dedicated, specialized instability control systems.

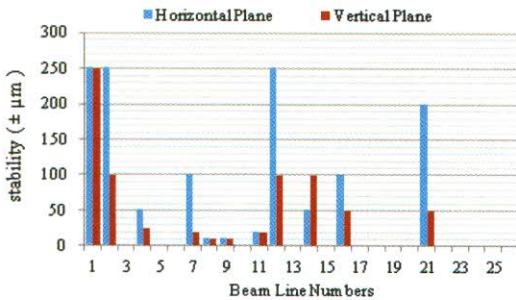


Fig. T.2.2: The stability requirement at source point in some of the Indus-2 beam lines

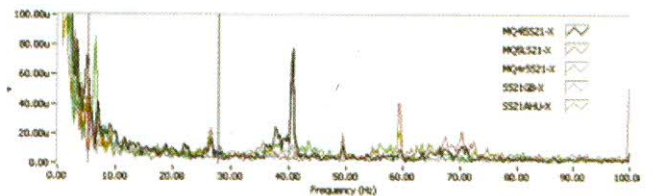
Typical beam stability requirements in SRS

The beam stability requirements for synchrotron radiation sources depend upon the sensitivity of 'photon-sample interaction and experimental setup' to beam parameter fluctuations. The beam line optical component configuration, photon beam properties, type of detector, sample characteristics and experiment method are the main factors that dictate this sensitivity dependence. Fig. T.2.2 shows the typical stability requirement for some of the existing and upcoming beamlines of Indus-2 in horizontal and vertical plane. Seeing the vastness of experiments that can be performed on different beamlines in third generation SRS, another widely accepted approximate stability requirement commonly considered is to have photon source point stability of 10% of the beam size and of angular divergence. For Indus-2, this dictates the stability requirement value for the tighter optics as $\pm 17\mu\text{m}$ in horizontal plane and to $\pm 3\mu\text{m}$ in vertical plane. Thus considering the scope of improved stability requirement by the upcoming beamlines, in Indus-2, the rms stability of $\pm 3\mu\text{m}$ is targeted for both the planes in final version of FOFB implementation.

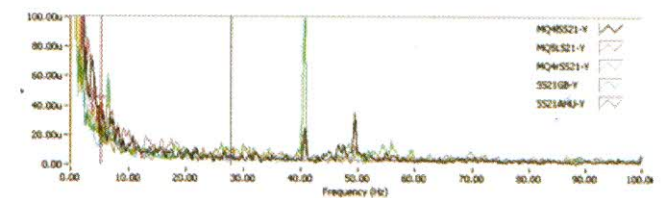
Typical bandwidth requirement of orbit correction

The bandwidth requirement for SOFB correction is primarily decided by the machine's physics design and is mainly limited by the slow corrector magnet system's

(corrector power supplies and corrector magnets) frequency response and the tolerable (beam survival ability) maximum orbit deviation pulse amplitude. In Indus-2 the measured fastest correction loop rate for SOFB is once every 14 seconds at 2.5Gev under present machine operating conditions whereas considering the stability of control loop the loop-rate of once every 20 seconds is normally applied. The bandwidth requirement for FOFB is governed by the presence of total noise in the system and the nature of its spectral contents.

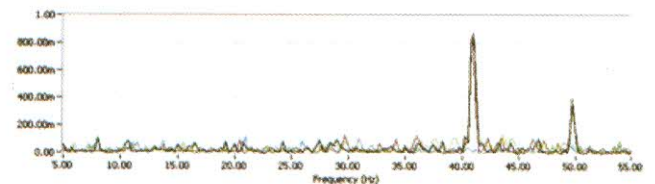


(a)

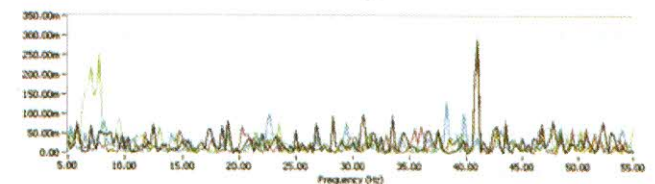


(b)

Fig. T.2.3: The vibration spectrum of SS2 magnets in Indus-2 (a) horizontal (b) vertical



(a)



(b)

Fig. T.2.4: Coherence between girder and magnet vibrations: (a) horizontal (b) vertical plane of SS2 magnets in Indus-2

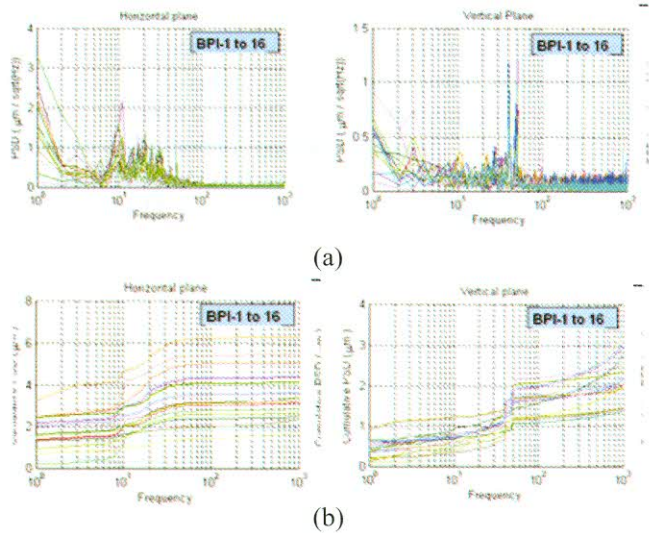


Fig. T.2.5: Noise spectral analyses (a) shows the PSD of 16 BPIs in Indus-2, and (b) the integrated PSD for the same

Fig. T.2.3 and T.2.4 show the vibration spectra measured at SS2 magnets in Indus-2 along with the coherence between the girder and magnets [3]. From this data, it can be seen that the ground vibrations at 41.5Hz can easily pass through girders in Indus-2. Thus the best possible efforts are required to be done towards passively damping of ground noise around 41.5Hz as well as this frequency must be covered by the FOFB system bandwidth.

The integrated displacement and power spectrum of the BPI data taken at 16 BPI locations in Indus-2 are shown in Fig. T.2.5. From integrated displacement graph, Fig. T.2.5(b), it can be seen that the major noise contribution is from frequency components up to 100 Hz. From this, the upper 3dB cutoff frequency for FOFB in Indus-2 is selected as 100Hz.

Settings resolution (DAC resolution) requirement

The choice of orbit correction setting resolution (DAC resolution) depends on physics design of the machine, the maximum amplitude of noise within the correction band, control system architecture (mutual error correction rate between SOFB and FOFB, mutual correction frequency band sharing topology), maximum corrector strength required, corrector power supply stability & resolution and the selected electronics component/ hardware for this purpose.

Table T.2.3: Indus-2 FOFB system design specifications

Sr No	Parameter	Value
1	RMS stability	$\pm 3\mu\text{m} @ 2.5\text{GeV}$
2	Corrector strength	$\pm 25\mu\text{rad} @ 2.5\text{GeV}$
3	Correction BW (3dB)	100Hz
4	Settings resolution	16bit
5	Power supply stability	50ppm
6	Control loop rate	> 4KHz

Table T.2.3 lists the DAC resolution value ranging from 16bits to 24 bit adopted by fast orbit feedback control systems at different synchrotron radiation sources. Considering the above stated factors for Indus-2, the DAC resolution of 16 bits is selected for implementation. All other FOFB design parameters are calculated based on the stability, bandwidth and resolution requirements. Table T.2.3 lists some of these major design specifications adopted for Indus-2 FOFB system.

Global SOFB systems

Mostly global slow orbit feedback control system uses the slow correctors (Iron core steering magnets) used for COD correction in the machine to correct the slow occurring beam vibrations. These correctors being iron core provide relatively larger correction kick ($\sim \pm 1.2\text{mrad}$ in Indus-2) to the beam as compared to fast corrector magnets ($\sim \pm 25\mu\text{rad}$ in Indus-2). Thus this system supports FOFB system by continuously maintaining the electron orbit within the dynamic range of FOFB corrections. Along with serving the orbit stability requirements, these also provide operators the facility for reference orbit definitions and local bump corrector. Fig. T.2.6 shows the block diagram of SOFB system at Indus-2.

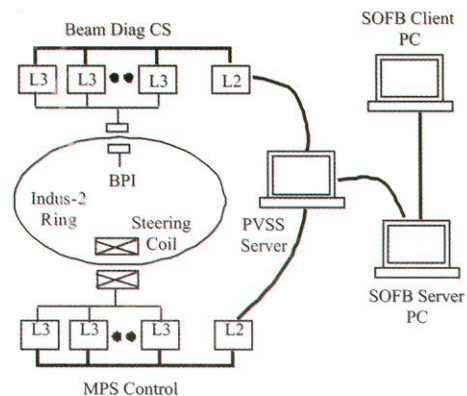


Fig.T.2.6: Block diagram of SOFB system for Indus-2

This system comprises of reading of beam position data from 56 beam position indicators (BPI) in each plane (vertical and horizontal) and then calculating the correction values to be applied to 40 correctors in vertical plane and 48 correctors in horizontal plane using PID algorithm with parameter decoupling matrix calculated using singular value decomposition. With the developed SOFB system, now the naturally occurring beam drift of order of $\pm 300\mu\text{m}$ has been brought down to $\pm 30\mu\text{m}$ in both the planes. Fig. T.2.7 shows the orbit drift in vertical plane for the SOFB ON and SOFB OFF cases.

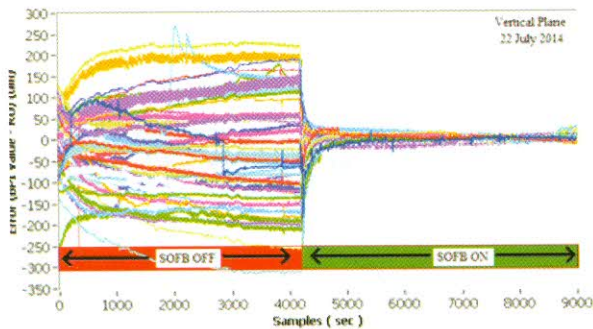


Fig. T.2.7: Orbit drift in vertical plane with SOFB OFF and ON

Local FOFB system

In local feedback control system the beam position variations occurring at a particular location are targeted for correction. In this scheme, 3 to 4 corrector magnets are powered to produce local bump with closed orbit in order to lock the orbit to one or two beam position monitors. Here the bump is local and hence the orbit outside the bump is unaffected. As both the sensors and actuators are in near vicinity this scheme enjoys the advantage of easy implementation, simple controller structure and potential for very fast correction rates. Also in this scheme the beam position obtained from photon BPIs installed in the beam lines are used these days to get very precise light spot control at sample. The interference avoidance between parallel running multiple local loops is the main challenge in this type of scheme as with slight change in the systems transfer function, the bump closure condition disrupts, resulting in a leaking bump.

For evaluating the performance of the selected hardware for FOFB system and to gain experience for implementing the fast feedback control loops in MIMO systems, it was decided to implement a prototype local FOFB system on BL-8 of Indus-2 and then refine the specifications according to the test

results for the second phase. The local FOFB system is implemented on BL-8 of Indus-2 as per the block diagram shown in Fig T.2.8.

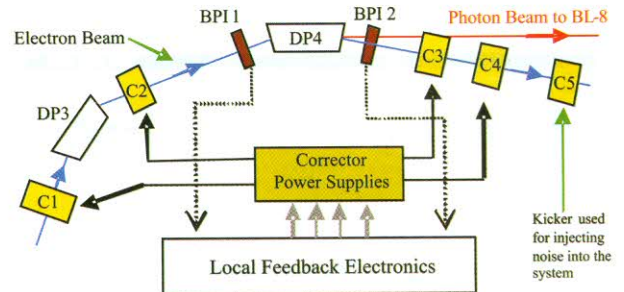


Fig.T.2.8: Block diagram of local FOFB system on BL-8

Beam position local to DP4 is sensed using BPI1 and BPI2. Libera BPI in libera grouping configuration is used along with the developed LabVIEW® RT PXI driver for getting the beam position data with 10K samples/second data rate (Fig. T.2.9). Five air core correctors (Fig. T.2.10) [4] are used as actuators, out of which C1, C2, C3, C4 are used for corrective closed bump generation and C5 is used for injecting the known noise into the system for systems characterization.

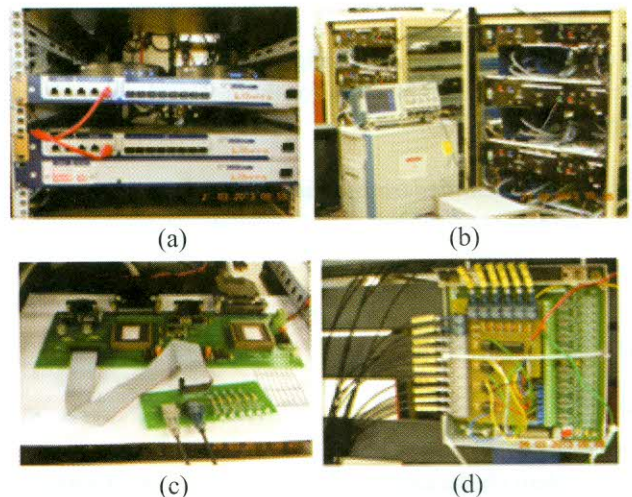
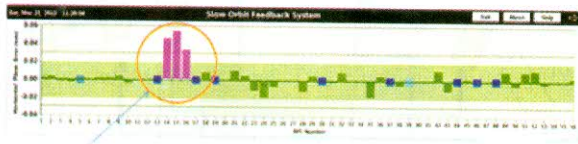


Fig. T.2.9: FOFB components (a) Libera BPIs units and (b) Fast corrector power supply (c) P/S communication module

Sr.No	Parameter	Value
1	Type	combined
2	Strength (H)	$\pm 30\mu\text{rad}$
3	Strength (V)	$\pm 40\mu\text{rad}$
4	Typical Freq	200Hz
5	Typical Current	$\pm 10\text{A}$
6	phase lag (200Hz)	$\sim 5^\circ$ to $\sim 7^\circ$

Fig. T.2.10: Fast Corrector magnet (a) Picture (b) specification

Starting with the initial model derived values of coefficients for 'four kicker closed orbit bump', the final inverse response matrix coefficient values were iteratively derived with online bump closure validation (Fig. T.2.11).



Closed Local Bump at BL-8

Fig.T.2.11 Local bump closure validation

Using this decoupling matrix for each plane, the '4 input 2 output system' is converted to two independent control channels with control schematic shown in Fig. T.2.12.

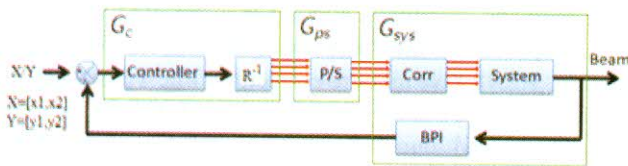


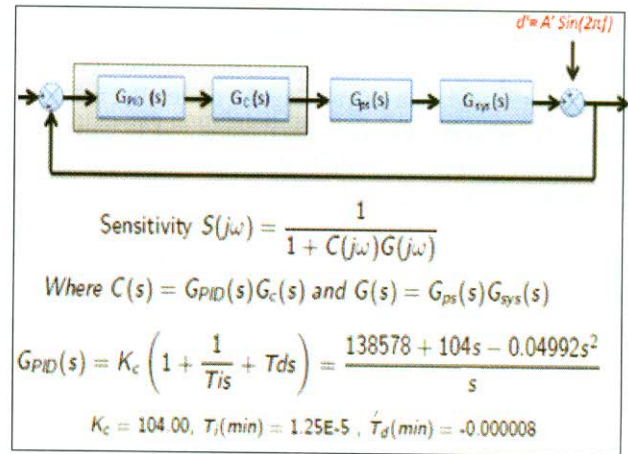
Fig. T.2.12: Control schematic for individual decoupled channel

Through system identification experiments performed on the system in open loop configuration (with step stimulus) the systems transfer function for these virtual channels are derived (Table T.2.4).

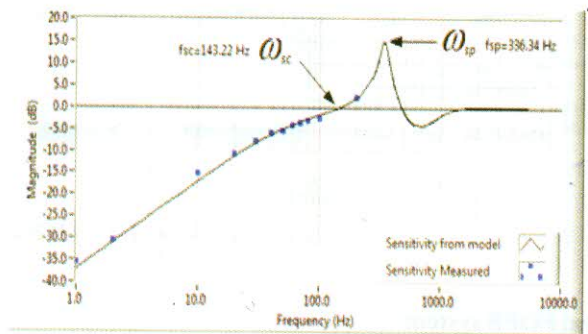
Table T.2.4: Identified transfer function of different blocks for one channel in each plane

	Hplane	Vplane
G_c	$e^{-0.0002}$	$e^{-0.0002}$
G_{PID}	$\frac{1.00076}{(1 + 3.04E - 4s + 6.19E - 8s^2)}$	$\frac{0.941(1 + 5.98E - 4s)}{(1 + 2.69E - 4s + 7.16E - 8s^2)}$
G_{sys}	$\frac{e^{-0.0003} 0.003(1 - 2.63E - 4s)(1 - 5.31E - 5s)}{(1 + 2.80E - 4s + 6.00E - 8s^2)}$	$\frac{e^{-0.0003} 0.00383(1 + 2.37E - 1s)}{(1 + 1.48E - 3s)(1 + 5.140E - 4s + 2.36E - 7s^2)}$

System characterization in closed loop for disturbance rejection is performed through experiments by injecting the sinusoidal disturbance in beam using a separate corrector (C5 in Fig. T.2.8) downstream the correction point. Fig. T.2.13 shows the system configuration for these experiments and the characterization results in horizontal plane.



(a)



(b)

Fig. T.2.13: Horizontal plane control loop characterization (a) system configuration, (b) measured noise sensitivity

Simulation studies done over system model built using the experimentally identified systems transfer functions showed that the developed hardware can provide the required attenuation at 100Hz (Fig. T.2.14). Based on these simulations, the hardware specifications are improved for power supply and communication interface. This will help to tune the controller for good gain margin (6dB to 14dB) and phase margin (30° to 45°) values. This will also increase the sensitivity peak frequency with reduced gain as desired.

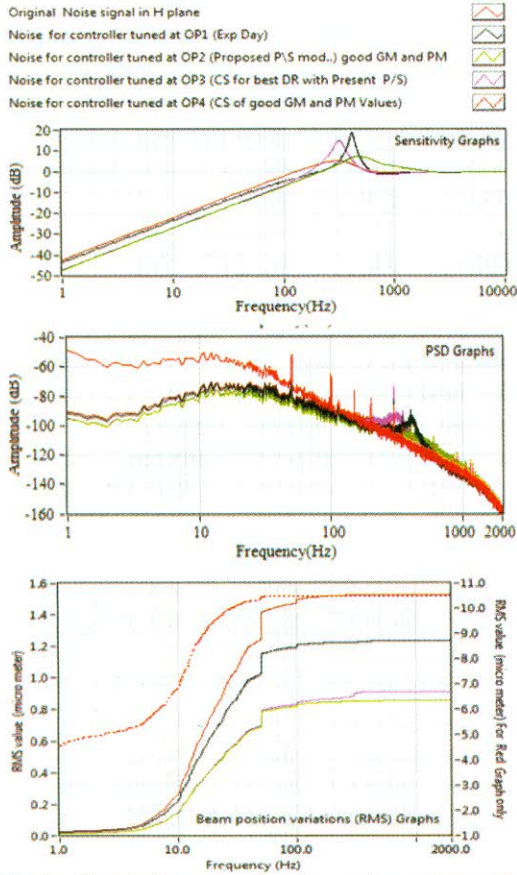


Fig.T.2.14: Simulation results for noise attenuation and achievable beam stability with different controller tuning with old and new proposed fast corrector power supply characteristics

This system successfully lowered down the naturally occurring beam position variation from $\pm 30\mu\text{m}$ pk-pk (H plane), $\pm 10\mu\text{m}$ pk-pk (V plane) to $\pm 3\mu\text{m}$ pk-pk in both the planes (Fig. T.2.15).

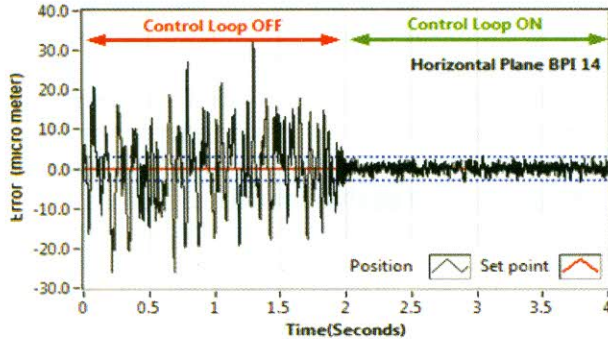


Fig. T.2.15: Beam position error in horizontal plane with Local FOFB OFF and ON cases (blue lines show $\pm 3\mu\text{m}$ band)

Global FOFB system

Global FOFB systems are targeted towards mitigation of beam movement in frequency range 1Hz to 200Hz. This scheme in principle uses control concepts similar to SOFB scheme but through altogether new challenges in its implementation. For linear system case the orbit shift, $\Delta\vec{y}$, from multiple steering magnets changes $\Delta\vec{\theta}$, can be written in matrix form as:

$$\Delta\vec{y} = M\Delta\vec{\theta} \quad (1)$$

Here M is the orbit response matrix. This response matrix is measured by applying a small stimulus signal on each actuator and then measuring its effect on beam position all along the ring. Global FOFB is a MIMO type of system. The common practice is to break the MIMO problem to n parallel single-input single-output feedback control loops using M^{-1} as decoupling matrix. Mostly the M is singular or close to singular, so it has no well defined inverse. To deal with this problem various algorithms have been developed out of which the singular value decomposition (SVD) has emerged as the most popular and is generally used in orbit feedback corrections. Any matrix M can be represented with SVD as:

$$M = \sum_{k=1}^n \vec{u}_k w_k \vec{v}_k^T \quad (2)$$

where \vec{u}_k is a set of orthonormal steering magnet vectors, \vec{v}_k is a corresponding set of orthonormal BPI vectors and w_k are the singular values of the matrix M . The inverse matrix is then calculated as:

$$M^{-1} = \sum \vec{v}_k \sigma_k \vec{u}_k^T, \quad \sigma_k = \begin{cases} 0 & \text{for } w_k < \epsilon \\ \frac{1}{w_k} & \text{for } w_k \geq \epsilon \end{cases} \quad (3)$$

Where ϵ is the parameter that provides a control to user for deciding the quality of pseudo-inverse. This plays important role in orbit feedback systems as by selecting the suitable value for ϵ the inverse contribution resulting from small value w_k terms can be omitted. This is beneficial as small w_k generate large steering magnet strength changes with little improvement in orbit corrections. Also removing the small w_k tends to filter out the effect of erroneous BPI data as erroneous BPI data gives a larger contribution to \vec{u}_k with small w_k [5].

In this method with the suitable w_k terms selected, the ratio of largest to smallest singular values indicates how sensitive the solution of the system is to small changes in the sensors. For most of the machines this is large denoting the ill-conditioned system. Tikhonov regularization [6] method is

utilized for conditioning of the matrix by the relatively new machines. This method scales the singular values when calculating the pseudo-inverse by using the modified σ_k in place of σ_k in eq.(3) given as:

$$\sigma'_k = \begin{cases} 0 & \text{for } w_k < \epsilon \\ \frac{w_k}{w_k^2 + \mu} & \text{for } w_k \geq \epsilon \end{cases} \quad (4)$$

Where μ is the parameter selected by the user. This scaling of singular values has the effect of changing the speed of correction of the respective modes in a feedback system with integral action.

Using this inverse response matrix as decoupling matrix, the common practice is to use the PI type controller for the parallel SISO feedback loops. Mostly the problem of actuator limitations (saturation and slew rate) is treated with anti-windup schemes (Fig. T.2.16 shows one of such anti-windup scheme) in control loop to prevent overshooting in closed-loop response when large current demands are sent to the power supplies.

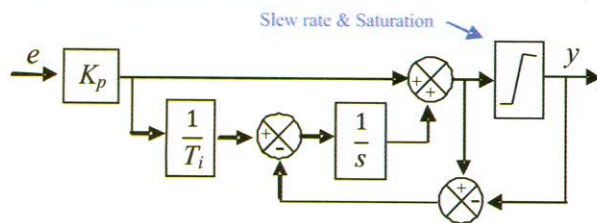


Fig.T.2.16: Block diagram for PI anti-windup scheme

Another advanced controller tried for orbit control is the Internal Model Control (IMC). The benefit of this scheme is its ability to handle the system delays (as in global FOFB, the controller delays are significant) but requires the accurate system model knowledge. To attain the submicron level stability requirements being posed by the coming high brilliance SR machines, the current research in this area is aiming towards the controller design that provides compensation in frequency domain at each eigenmode level, that is, a dynamic controller on each transformed corrector coordinate in mode space instead of the real corrector setpoints. The challenge for such individual eigenmode compensation is that the feedback system needs to finish much more calculations within the time budget of the fast orbit feedback system. Implementation wise the focus is towards FPGA based embedded distributed computing to overcome this calculation time limitation.

Seeing the possible benefit of using artificial intelligence based control systems for accelerator tuning and operations [7, 8], the efforts are also being done towards

getting benefits of distributed artificial intelligence in orbit control systems [9]. Further to this with the ongoing research towards new system identification methods for networked control systems [10], the field of global orbit feedback is going to evolve towards incorporating adaptive control concepts to fulfill the increasing demand of beam stability by the user community in near future.

Implementation wise, following are the major challenges posed in the global FOFB systems.

1. Identical characteristics for all P/S: unlike the global SOFB, in global FOFB, the correction interval is small as compared to the system settling time. Thus the assumption that the response matrix represents the system (within tolerance) must be satisfied not only at steady state but also during the transition period for correctors to reach to their set values. This requires the additional mechanism in control system for assisting P/S tuning & verification in field with online data along with careful P/S design.
2. Synchronous settings for all P/S: the data to all power supplies in one plane are required to be updated in synchronous manner with very small jitter (<50µs). This is achieved with custom communication modules with protocol implemented in FPGA logic for error handling and decoding (frame time ~6µs).
3. Channel to channel isolation and noise free communication: this is achieved by adopting optical fiber based networks for communication.
4. BPI data pre-filtering, scaling and corrector current calculation within short time budget (< 60µs): this is achieved with distributed calculation in FPGA / real-time operating system environment.
5. BPI data parsing, sharing between different nodes and data grouping (<40 µs): this is achieved through custom developed BPI server modules in real-time operating system environment and reflective memory based data sharing methods.
6. Synchronous beam position data capturing and transmission at 10 KHz rate: this is achieved with Digital BPIs (e.g. Libera) configured in libera grouping configuration over gigabit Ethernet.
7. Both transient (Transfer Function) and steady state system response matrix measurement: this is achieved by incorporating the software tools for system identification (SI) in control system GUI for stimulus generation, SI experiment conduction configuration with data logging and automatic transfer function extraction features.

8. Real-time Controller tuning and system performance verification: this is achieved by providing the features for real-time beam position variation data presentation for analysis in both time domain as well as frequency domain in the control system GUI.
9. System stability: this is achieved by incorporating the logic based controller supervision for automatic handling of errors arising out of controller induced instability, corrector saturation, power supply tripping, communication errors and loop start preconditions.
10. Simultaneous global SOFB and global FOFB loop operation: The global FOFB systems exhibit fast correction characteristics but cover very small dynamic range, thus its continuous operation without saturating the fast correctors requires, the average electron orbit, always to be maintained near center of its dynamic range. This is achieved through maintaining the logical supervised operation of FOFB by the SOFB application where SOFB system as master controls the operation of FOFB system according to the system's current state and future predicted beam movements to be executed by SOFB system.

Indus-2 Global FOFB system

In Indus-2 the global FOFB system is being implemented in phases. In its first phase the FOFB system with 16 BPIs and 16 fast correctors is developed for both the planes. In the second phase this scheme will be extended to the full 56 BPI and 32 corrector version for both the planes. Fig. T.2.17 gives the block diagram for global FOFB system at Indus-2.

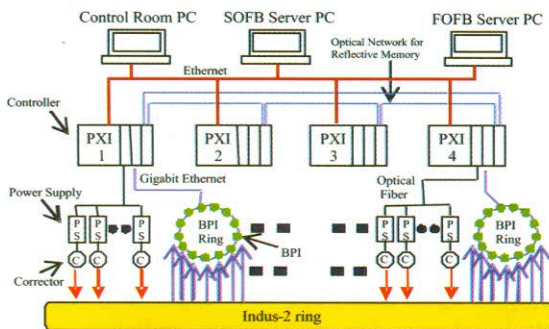


Fig. T.2.17: Block diagram for FOFB system at Indus-2

There are 16 Digital BPI units in the ring and configured to make a single libera group. There are four such libera groups each connected to one PXI controller unit. There are 32 fast corrector power supply (with improved transfer function) connected using improved communication interface (Fig.T.2.18) to each PXI controller unit. The beam

position data coming from each digital BPI group over Gigabit Ethernet link to PXI units are first decoded, scaled, qualified and then shared among all 4 PXI controller units using dedicated reflective memory network. The design specifications for Indus-2 FOFB system are listed at Table T.2.2. The first phase of FOFB system uses PI control algorithm with SVD based inverse matrix for parameter decoupling. Fig.T.2.19 shows the snapshot of GUI panel with identified system model and transfer function for each channel in horizontal plane. Fig. T.2.20 shows the integrated power spectrum (vector integration for all 16BPIs) in horizontal plane with, and without correction cases.

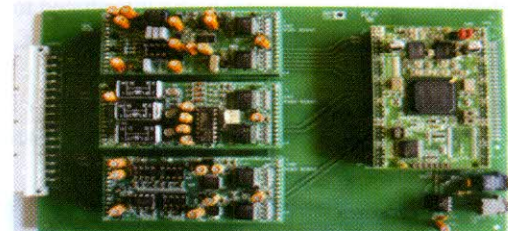


Fig.T.2.18: Developed hardware for improved P/S interface

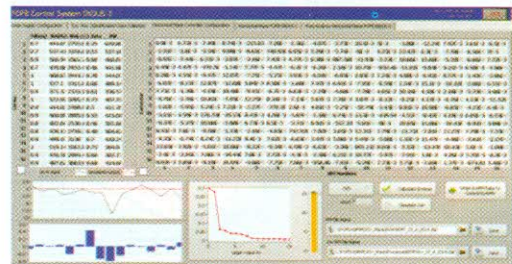


Fig.T.2.19: GUI snapshot of system identification tab in FOFB

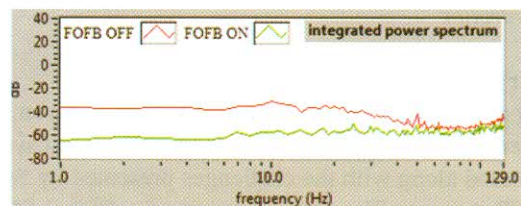


Fig. T.2.20: Integrated power spectrum in horizontal plane

This developed system successfully confined the beam position variations (pk-pk) from $\sim \pm 40\mu\text{m}$ to $\sim \pm 12\mu\text{m}$ in horizontal plane and from $\sim \pm 30\mu\text{m}$ to $\sim \pm 10\mu\text{m}$ in vertical plane. In this first phase development, noise attenuation of $\sim 5\text{dB}$ at 50Hz has been achieved in both the planes.

Average orbit drift (horizontal plane) correction using RF frequency compensation

The average orbit drift (in horizontal plane) arising due to the path length changes cannot be corrected using the

corrector magnets. Thus for correcting these effects, average orbit correction with RF frequency compensation is usually employed. One such system has been developed for Indus-2 and is in its testing phase.

Future research directions in orbit control systems

The orbit control system represents the distributed MIMO type fast feedback systems. Presently the identified linear system model is utilized for systems controller design and decoupling. There is enormous performance improvement possibility in SOFB and FOFB with the artificial intelligence based adaptive controller design and the model predictive controller concepts being introduced to this field (Fig. T.2.21). But these require some of the implementation issues to be solved, particularly the calculation delay constraints in real-time. For this, FPGA based dedicated hardware calculation is the current method which researchers are working upon.

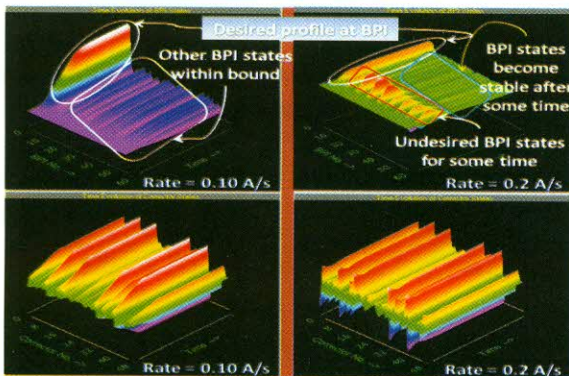


Fig. T.2.21: Simulation results for Indus-2 SOFB showing evolutions of states for BPI and correctors for both PI and MPC controller

Summary

An overview of the orbit control system is given. The parameters affecting different orbit feedback control system are discussed along with the challenges presented by SOFB and FOFB systems. The control systems for Global SOFB, Local FOFB and Global FOFB first phase are developed and installed at Indus-2. All the developed orbit control systems at Indus-2 are operating successfully to fulfill the present user demands for beam stability. The future improvements in these systems are aimed towards fulfilling the beam stability demands expected by the new upcoming beam lines.

Acknowledgment

The successful implementation of FOFB at Indus-2 has been made possible by expertise, skills and dedicated hard-work from all the members of FOFB team comprising of

members from Power Supplies & Industrial Accelerator Division, Accelerator Magnet Technology Division, Beam Diagnostics Section, Beam Dynamics Lab, Indus Synchrotron Utilization Division and Indus Operations & Alignment Lab. The vibration study at Indus-2 is carried out by Vibration Laboratory Section, RED, BARC, Mumbai.

REFERENCES

- 1] R.O. Hettel, Beam Stability Issues at Light Sources, 25th ICFA Advanced Beam Dynamics Workshop SSILS, SSRC Shanghai, China, 2002
- 2] M.Boge, Achieving Sub-micron Stability in Light Sources, In Proceedings of EPAC 2004, Lucerne, Switzerland, 2004
- 3] S.K. Sinha, K.K. Meher and A. Rama Rao, Vibration measurement on INDUS-2 Equipments, Internal report, BARC/RRCAT, 2013
- 4] S. Das, K. Sreeramulu, A. Kumar, B. Srinivasan, K. Singh, B. Singh, A. K. Mishra and R.S. Shinde, development of fast corrector magnets for fast orbit feedback system of Indus-2, Indian Particle Accelerator Conference, 19-22 November 2013, Kolkata, India, 2013
- 5] J. Safranek, Orbit control at synchrotron light sources, ICALEPCS 1999, Trieste, Italy, 1999
- 6] J. Rowland, M.G. Abbott, J.A. Dobbing, M.T. Heron, I. Martin, G. Rehm, I. Uzun and S.R. Duncan, Status of the Diamond fast orbit feedback systems, ICALEPCS07, Knoxville, Tennessee, USA, 2007
- 7] R.P. Yadav, P. Fatnani, P.V. Varde, P.S.V. Nataraj, A multi-agent based control scheme for accelerator pre-injector and transport line for enhancement of accelerator operations, Online journal Elixir Comp. Sci. & Engg. Vol.44, pp.7405-7410, 2012
- 8] R.P. Yadav, P.V. Varde, P.S.V. Nataraj, P. Fatnani, C.P. Navathe, Model-based Tracking for Agent-based Control Systems in the Case of Sensor Failures, International Journal of Automation and Computing, Vol.9, No.6, pp.561-569, 2012
- 9] R.P. Yadav, P.V. Varde, P.S.V. Nataraj, P. Fatnani, Intelligent agent based operator support and beam orbit control scheme for synchrotron radiation sources, International Journal of Advanced Science and Technology, Vol.52, pp.11-34, 2013
- 10] R.P. Yadav, P. V. Varde, A. Chauhan, P. Fatnani, Feedback-Based Critical Parameter Estimation for First Order Plus Dead Time Type Plant in Networked Control System Configuration, International Journal of Modeling, Simulation and Scientific Computing Vol.2, No.3, pp. 375-391, 2011